

A Sustainability Roadmap for C³

**Martin Breidenbach, Brendon Bullard, Emilio Alessandro Nanni, Dimitrios Ntounis[†],
Caterina Vernieri**

SLAC National Accelerator Laboratory [†] & Stanford University

ABSTRACT: The particle physics community has agreed that an electron-positron collider is the next step for continued progress in this field, giving a unique opportunity for a detailed study of the Higgs boson. Several proposals are current under evaluation of the international community. Any large particle accelerator will be an energy consumer and so, today, we must be concerned about its impact on the environment. This paper evaluates the carbon impact of the construction and operations of one of these Higgs factory proposals, the Cool Copper Collider (C³). It introduces several strategies to lower the carbon impact of the accelerator. It proposes a metric to compare the carbon costs of Higgs factories, balancing physics reach, energy needs, and carbon footprint for both construction and operations, and compares the various Higgs factory proposals within this framework. For C³, the compact 8 km footprint and the possibility for cut-and-cover construction greatly reduce the dominant contribution from embodied carbon.

Contents

1	Introduction	1
2	Review of the C³ accelerator design	2
3	Comparison of Higgs factory physics reach	3
4	Power consumption and optimizations	6
5	Carbon impact of construction	8
6	Mitigation strategies for operations	11
7	Analysis of total carbon footprint	13
8	Conclusions	16
9	Acknowledgements	17
	Bibliography	17

1 Introduction

An electron-positron collider gives a unique opportunity to study the Higgs boson's properties with unprecedented precision and also provide an exceptionally clean environment to search for subtle new physics effects [1]. A number of different "Higgs factory" proposals, based on linear and circular colliders, are now under consideration. All of these provide e^+e^- collisions at center of mass energies in the range of 240-370 GeV, and some also are capable of reaching higher energies.

A high-energy particle collider is a large energy-consuming research facility. As such, it is important to balance its scientific importance against its environmental cost. The environmental impact of large accelerators has been analyzed in the recent Snowmass 2021 study [2] of the future of particle physics in the US [3–5]. The papers [4, 6–8] have examined the environmental cost of particular Higgs factory proposals, though often concentrating on particular elements of the total cost.

In this paper, we attempt a comprehensive evaluation of the carbon cost of the Cool Copper Collider (C³) Higgs factory proposal [9, 10] over its full lifetime, including costs from construction and from operation over the proposed timeline. The structure of this paper is as follows: in Section 2, we briefly review the design of C³. In Section 3, we review the physics reach for C³ and other Higgs factory proposals and introduce a metric for balancing carbon impact against the physics impact of

each proposal. In Section 4, we analyze the power costs of operation of C^3 and describe methods for modifying the power design of the accelerator that would lead to substantial savings with little impact on the physics performance. In Section 5, we analyze the carbon impact of the construction of C^3 and emphasize that cut-and-cover construction, as opposed to construction in a deep tunnel, has significant advantages. In Section 6, we discuss options for the source of electrical power for the C^3 laboratory. In Section 7, we bring these analyses together to estimate the total carbon footprint of C^3 . Using information from available studies and design reports, we estimate the carbon impact of other Higgs factory proposals and compare these to C^3 in the framework described in Section 3.

2 Review of the C^3 accelerator design

C^3 , recently proposed [9, 10], is a linear facility that will first operate at 250 GeV center-of-mass collisions. Immediately after, without further extension of the linac, it will run at 550 GeV with an RF power upgrade. The high energy operations will enable the exploration of the Higgs-top coupling, and provide direct access to the Higgs self-coupling with double Higgs production [10, 11]. Furthermore, the beam polarization, which exploits the strong dependence of electroweak processes on the chirality of the initial state particles, will offer unique insights into the underlying physics, acting as a new tool for discovery [12]. This offers C^3 a strong complementarity with proton and circular e^+e^- colliders, where beam polarization is not possible.

C^3 utilizes a radically different approach to linear accelerators to build a collider with high gradient and high RF efficiency, and thus lower capital and operating costs [13]. C^3 is based on a distributed coupling accelerator concept, running under liquid nitrogen (LN) [14], that has led to an optimized accelerating gradient and minimized breakdown problems with respect to earlier designs based on normal conducting technologies. This has yielded an overall optimization of the gradient at 70 and 120 MeV/m for the 250 GeV and 550 GeV operating points, respectively.[15]. Much higher energies are possible if length is not the major consideration. The fundamental C^3 parameters, assumed for the analysis in this paper, are shown in Table 1.

By far the major development to date is the actual distributed coupling accelerator structure. C^3 will use C-band (5.712 GHz) standing wave RF accelerating structures that are 1 m long. Each has an RF waveguide to bring power in, and in the more probable operating modes, splits RF power evenly between the beam and dissipation in the structure with 43% beam loading. Operating at 80 K brings the shunt impedance up to 300 M Ω /m, allowing for efficient operation at 120 MeV/m. These gradients have been demonstrated at C-band [16] and with an electron beam in an X-Band (11.424 GHz) structure on the SLAC XTA beamline [14]. The C-band structure has been tested at low power at SLAC and at high power without beam at Radiabeam [17]. The C^3 gradient results in a collider with a 550 GeV center-of-mass energy capability on an 8 km footprint.

A pre-conceptual design for the overall linac cryogenics has been developed that includes the design for the CryoModules. For the C^3 250 GeV and 550 GeV design, each linac will have 3 re-liquification cryoplants. LN will flow out along the linac in both directions, so there are 6 flow runs. The LN will be above the raft structures, with an initial velocity of ~ 0.03 m/s. The LN will cool the accelerator structures by nucleate boiling with a power density of 0.4 W/cm², producing saturated

vapor which counter-flows back to the cryoplant. Each cryo-run is about 450 meters in length. The vapor velocity near the cryoplant is ~ 3 m/s.

Parameter [Unit]	Value	
CM Energy [GeV]	250	550
Luminosity [$1 \cdot 10^{34}$]	1.3	2.4
Num. Bunches per Train	133-200	75
Train Rep. Rate [Hz]	120	120
Bunch Spacing [ns]	5.3-3.5*	3.5
Site Power[MW]	150	175
Beam Power [MW]	2.1	2.45
Gradient [MeV/m]	70	120
Geometric Gradient [MeV/m]	63	108
RF Pulse Length [ns]	700	250
Shunt Impedance [$M\Omega/m$]	300	300
Length [km]	8	8

Table 1: Target beam parameters for C^3 . (*) Beam dynamics and structure optimization studies are ongoing: the injected charge range is between 0.7-1 nC with a bunch spacing ranging between 3.5 to 5.3 ns and final horizontal beam size ranging between 156.7 nm and 182 nm, without changes to the instantaneous luminosity. Accelerating structure optimization studies include varying the a/λ from 0.05 to 0.07 with $\pi-2\pi/3$ phase advance[13] to reduce the longitudinal wakefield and preserve the shunt impedance.

3 Comparison of Higgs factory physics reach

Among the e^+e^- colliders being evaluated by the community, the International Linear Collider (ILC) [12, 18], based on superconducting RF technology, has the most advanced design [19], and the ILC is currently under consideration for construction in Japan. CERN is pursuing as its main strategy a large circular collider, the FCC [20], and China is planning a similar circular collider, the CEPC [21]. Each of these circular colliders would require a tunnel with circumference of the order of 100 km to limit synchrotron radiation. Still, though, the expected instantaneous luminosity drops off significantly above center-of-mass energies of 350–400 GeV. A different alternative is to construct a compact linear e^+e^- collider based on high gradient acceleration. CERN is also pursuing such a proposal, CLIC [22], that would operate at a collision energy of 380 GeV.

The carbon footprint of the proposed future Higgs factories should be assessed relative to the expected physics reach, which has been reviewed most recently in the context of the Snowmass Community process [1, 23]. The primary physics goal of a future Higgs factory is the determination of the total Higgs width and Higgs couplings with per-cent or sub-per-cent precision. A reasonable figure

of merit to gauge the physics reach of each machine is the expected level of precision for each of these measurements. We note that evaluating the projected measurement precision accounts for the fact that different beam configurations (center-of-mass energy and beam polarization) have a strong impact on the physics reach of each of those machines. These differences in precision are not accounted for when comparing the total number of Higgs bosons produced alone [1, 12].

The physics reach at e^+e^- colliders increases with the center-of-mass energy, since different Higgs boson production mechanisms become accessible. At 250 GeV center-of-mass energy operations the main Higgs boson production mechanism is associated production with a Z boson ($e^+e^- \rightarrow ZH$), enabling a model-independent determination of the Higgs boson total width. Higgs boson production via the W-boson fusion reaction $e^+e^- \rightarrow \nu\bar{\nu}H$ is accessible at $\sqrt{s} \sim 500$ GeV, where the only visible signals in the final state come from Higgs boson decays. This allows Higgs boson measurements governed by different systematic effects, complementary to the 250 GeV data, as well as opportunities to study effects such as separation of $H \rightarrow gg/b\bar{b}/c\bar{c}$ decays and CP violation in $H \rightarrow \tau^+\tau^-$ [12]. Importantly, at high center-of-mass energies, double Higgs boson production in the ZHH channel opens up, providing direct access to the Higgs boson self-coupling λ_3 . At circular machines, given the energy limitations, double Higgs boson production mechanisms are not accessible, thus allowing only for indirect and model-dependent measurements of λ_3 , through loop effects in single-Higgs production.

The use of longitudinal beam polarization offers unique advantages for effective precision measurements at a linear e^+e^- collider, since the interaction cross sections at an e^+e^- collider have strong dependencies on beam polarization. It has been demonstrated that at 250 GeV center-of-mass energy, the ultimate precision reach in the determination of Higgs couplings, through a Standard Model Effective Field Theory (SMEFT) analysis, for an integrated luminosity of 2 ab^{-1} with polarized beams, has comparable sensitivity to 5 ab^{-1} with unpolarized beams, with most of the gain coming from e^- polarization alone [24]. The main effect of beam polarization is to discriminate the effect of different SMEFT operators that contribute to the Higgs boson coupling. There is a similar gain of about a factor of 2.5 from discrimination of the effects of the operators contributing to the $WW\gamma$ and WWZ couplings, which also enter the SMEFT analysis. The positron polarization becomes more relevant at higher center-of-mass energies. For instance, W-boson fusion reactions, such as $e^+e^- \rightarrow \nu\bar{\nu}H$, proceed only from $e_L^-e_R^+$ initial states, providing a cross-section (or, equivalently, effective luminosity) enhancement of ~ 2.5 for typical polarizations foreseen at future linear e^+e^- machines [12]. Here positron polarization makes a significant contribution. This implies that the same number of Higgs bosons can be produced through this process with only $\sim 40\%$ of the integrated luminosity, compared to having unpolarized beams.

Moreover, beam polarization at high energy enables the suppression of relevant backgrounds, such as the dominant $e^+e^- \rightarrow W^+W^-$ background for positive (negative) electron (positron) beam polarization, increasing the signal-over-background ratio and allowing the precise measurement of the rate of other backgrounds, as well as the reduction of detector-related systematic uncertainties, with combined measurements of datasets with four distinct initial-state polarization configurations. These effects collectively indicate the increased precision reach that beam polarization provides for linear machines [12].

For these reasons, in this analysis we propose a comparison of the carbon footprint of collider

concepts relative to their expected precision in Higgs coupling measurements. Table 2 summarizes the projected relative precision for Higgs boson couplings measurements at each collider combined with projected results from the HL-LHC. As can be seen, the overall physics reach of all proposed Higgs factories is similar [1, 23] for the 240-250 GeV operations, and additional measurements become accessible for the higher center-of-mass energy runs at linear colliders. We also compare the Higgs Factory proposals in terms of total energy consumption and carbon emissions, for both construction activities and operations, with the latter being the most relevant number when evaluating each project’s impact on the global climate.

Relative Precision (%)	HL-LHC +					
	HL-LHC	CLIC-380	ILC-250/C ³ -250	ILC-500/C ³ -550	FCC 240/360	CEPC-240/360
hZZ	1.5	0.34	0.22	0.17	0.17	0.072
hWW	1.7	0.62	0.98	0.20	0.41	0.41
$hb\bar{b}$	3.7	0.98	1.06	0.50	0.64	0.44
$h\tau^+\tau^-$	3.4	1.26	1.03	0.58	0.66	0.49
hgg	2.5	1.36	1.32	0.82	0.89	0.61
$hc\bar{c}$	-	3.95	1.95	1.22	1.3	1.1
$h\gamma\gamma$	1.8	1.37	1.36	1.22	1.3	1.5
$h\gamma Z$	9.8	10.26	10.2	10.2	10	4.17
$h\mu^+\mu^-$	4.3	4.36	4.14	3.9	3.9	3.2
$ht\bar{t}$	3.4	3.14	3.12	2.82/1.41	3.1	3.1
hhh	0.5	0.50	0.49	0.20	0.33	-
Γ_{tot}	5.3	1.44	1.8	0.63	1.1	1.1
Weighted average	-	0.94	0.86	0.45	0.59	0.49

Table 2: Relative precision of Higgs coupling and total Higgs width measurements at future colliders when combined with HL-LHC. Results are from the Snowmass Report [23]. The FCC-ee numbers assume two IPs and 5 ab⁻¹ at 240 GeV and 1.5 ab⁻¹ at 365 GeV. The CEPC numbers also assume two IPs, but 20 ab⁻¹ at 240 GeV and 1 ab⁻¹ at 360 GeV. The top Yukawa coupling can be measured with almost double the precision C³ operated at 550 GeV compared to ILC operated at 500 GeV, due to the higher center-of-mass energy [25]. Nevertheless, in this study we assume the same precision for C³-550 as for ILC-500. Note that since there are no beyond the Standard Model decays allowed in this table, the width is constrained by the sum of the SM contributions. Entries with a dash (-) correspond to couplings that are out of reach ($hc\bar{c}$ at HL-LHC) or for which estimates were not yet available at the time of writing (hhh for CEPC). The weighted average shown in the last row has been calculated as explained in the text.

We then present an estimate of energy consumption and carbon footprint per unit of physics output. This is achieved by taking the average of the relative precision over all Higgs couplings, weighing them by the relative improvement in their measurement with respect to HL-LHC:

$$\left\langle \frac{\delta\kappa}{\kappa} \right\rangle = \frac{\sum_i w_i \left(\frac{\delta\kappa}{\kappa} \right)_i}{\sum_i w_i} \quad (3.1)$$

where the sum runs over the columns of Table 2 and the weight is defined as:

$$w = \frac{\left(\frac{\delta\kappa}{\kappa}\right)_{\text{HL-LHC}} - \left(\frac{\delta\kappa}{\kappa}\right)_{\text{HL-LHC+HF}}}{\left(\frac{\delta\kappa}{\kappa}\right)_{\text{HL-LHC+HF}}} \quad (3.2)$$

This definition weights measurements by their relative improvement over HL-LHC when combining the HL-LHC and future Higgs Factory (HF) results. Qualitatively, measurements that minimally improve those of HL-LHC are assigned weights near zero, while HF measurements with high precision or large improvement over HL-LHC are assigned larger weights. While other weighting schemes could be used, we argue that Equation 3.2 is unbiased towards the type of physics measurement (e.g. Yukawa, self-coupling, vector coupling) and it emphasises the individual strengths of each collider facility.

For the estimation of the weighted average precision, the $hc\bar{c}$ coupling was excluded, since there is no estimate for HL-LHC, whereas we assume that the hhh coupling for CEPC can be measured with the same precision as for FCC. The weighted average precision for each collider is given in the last row of Table 2.

4 Power consumption and optimizations

The most obvious way to reduce the carbon impact of a major facility is to minimize the amount of power that it consumes, thereby minimizing the associated emissions from energy production. This is firmly within the means of the facility designers and crucially does not rely on grid electrification. The nominal operating parameters for C³-250 are given in Table 3.

Parameter [Unit]	Value
Temperature [K]	80
Beam Loading [%]	45
Gradient [MeV/m]	70
Flat Top Pulse Length [μ s]	0.7
Total Beam Power [MW]	4
Total RF Power [MW]	18
Heat Load at Cryogenic Temperature [MW]	9
Electrical Power for RF [MW]	40
Electrical Power For Cryo-Cooler [MW]	60
Accelerator Complex Power [MW]	≈ 50
Site Power [MW]	≈ 150

Table 3: Estimated power consumption values for C³-250 at nominal luminosity.

Several avenues can be pursued to optimize operational power requirements. Improvements in luminosity or reduction in power consumption are possible through the development of ancillary

technology by increasing the RF source efficiency, increasing the efficiency of powering the accelerating structures or modification of beam parameters to increase luminosity. At present the main linac requires ~ 100 MW of power with 40 MW for the RF sources and 60 MW for the cryogenics.

For the RF sources, the C^3 concept utilizes an overall RF system efficiency of 50% which is in line with present high power RF sources that are designed with efficiency in mind. However, significant advances in modern design techniques for klystrons are increasing the klystron amplifier's ultimate efficiency significantly with the inclusion of higher order mode cavities, multi-cell outputs and advanced multi-dimensional computational tools. For example, designs now exist for a 50 MW class RF source[26] approaching an amplifier efficiency of 70%. Multi-beam RF sources, reducing the beam perveance, have advanced design efforts exceeding 80% efficiency[27]. These results reinforce modern understanding on the limits of klystron efficiency [28, 29] which indicate a klystron amplifier efficiency of 70-80% is possible, leading to an overall RF source efficiency of 65%.

RF pulse compression, presently not in the C^3 baseline, is also a well known technique for powering high gradient structures. For C^3 , pulse compression is particularly useful due to the impact of power loss at cryogenic temperatures and due to the relatively long fill time for a copper structure operating at cryogenic temperatures. In a previous study[13], it was found that low factors of pulse compression, which preserves RF efficiency in the compressor[30], improves the overall efficiency of the system by 30%. Recently, additional efforts have been made to realize the extremely high Q cavities required for pulse compression with cryogenically cooled RF structures [31, 32]; these include concepts operating at room temperature and inside the cryostat at 80 K.

For the baseline C^3 design [9, 10] we anticipate operation with 700 ns and 250 ns flat tops respectively for gradients of 70 and 120 MeV/m and a constant power dissipation of 2.5 kW/m at 120 Hz. Figure 1 and Figure 2 show the RF power, dissipated energy and gradient during the pulse. While these flat top lengths were selected to limit the challenges of breakdown, increasing the flat top length and reducing the repetition rate should be investigated in order to reduce the thermal load on the linac. At present, the thermal balance between the structure fill/dump time and the flat top is approximately 50% (equal thermal load). If we were to extend the flat top lengths by a factor of two and reduce the repetition rate by a factor of two, the thermal dissipation in the main linac would decrease by 25%. This improvement would have little effect on the overall design of the accelerator, and would be acceptable if the breakdown rates remain low enough. Proving that this is possible will require high gradient testing of structures with 1400 ns and 500 ns respectively.

The beam current of C^3 is relatively low thanks to the large bunch spacing and efficient accelerating structures. One could pursue the possibility of reducing the bunch spacing to increase the current. However, this will require compatibility studies with the detector design. Here we consider the scenario where the bunch spacing is reduced by a factor of two. This would keep a bunch spacing of >1 ns for both C^3 -250/550, resulting in a decrease of 25% for the cryogenics power. The RF power required would only decrease by 20% because the peak RF power required would be slightly higher during the RF pulse flat top to compensate for the additional current.

We note that these approaches can all be combined for mutual benefit as shown in the last row of Table 4. The demonstration R&D plan [11] will be able to investigate these approaches and lead to potential power savings.

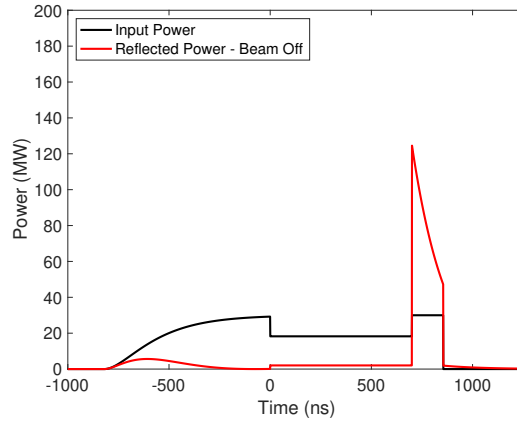


Figure 1: Forward and reflected power for one meter of structure when operating at 70 MeV/m. RF pulse is shown in the absence of beam. With beam the flat top power is constant at 30 MW.

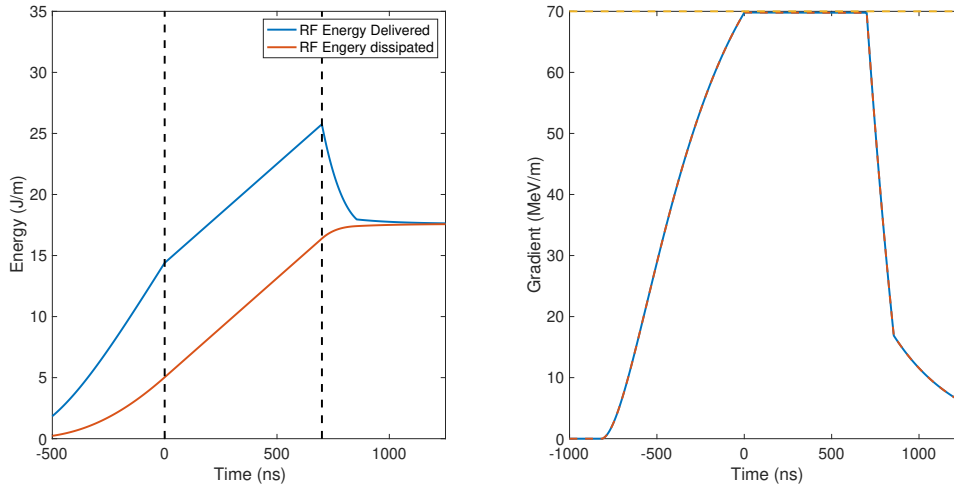


Figure 2: Dissipated energy per pulse per meter and the time domain gradient in the structure for a 70 MeV/m flat top for 700 ns.

5 Carbon impact of construction

Under the assumption that the electric grid will be successfully de-carbonized by 2040, as it is the goal of many international climate plans, then construction, rather than operations, may well dominate the climate impact of a new particle physics facility [5]. For FCC it is projected that the whole accelerator complex¹ will have a carbon impact similar to that of the redevelopment of a neighbourhood of a major city [5]. This indicates that the environmental impact of any future collider facility is going to receive

¹The main tunnel plus the additional buildings on the site, the materials for the accelerator and detectors, assuming a main tunnel length of 97.7 km (the updated FCC design anticipates 91 km).

Scenario	RF System (MW)	Cryogenics (MW)	Total (MW)	Reduction (MW)
Baseline 250 GeV	40	60	100	-
RF Source Efficiency Increased 15%	31	60	91	9
RF Pulse Compression	28	42	70	30
Double Flat Top	30	45	75	25
Halve Bunch Spacing	34	45	79	21
All Scenarios Combined	13	24	37	63

Table 4: Power savings with adjustment in main linac design and beam parameters. For 550 GeV the percentage savings would be unchanged for a combined 79 MW reduction in electrical power from the nominal 125 MW for the main linac.

the same scrutiny as that of a major urban construction project. The bottom-up analysis in [5] derives an estimate of global warming potential (GWP) for the main tunnel material (concrete) manufacture alone to be equivalent to the release of 237 ktons of CO₂ (CO₂e). An alternative top-down analysis is instead dependent on the character of the earth to be excavated, leading to estimates ranging from 5-10 kton CO₂e/km of tunnel construction and total emissions of 489-978 kton CO₂e².

A life cycle assessment of the ILC and CLIC accelerator facilities is being performed by ARUP [8] to evaluate their holistic GWP, so far providing a detailed environmental impact analysis of construction. The components of construction are divided into classes: raw material supply, material transport, material manufacture, material transport to work site, and construction process. These are labelled A1 through A5, where A1-A3 are grouped as materials emissions and A4-A5 are grouped as transport and construction process emissions. The total GWP for ILC and CLIC is taken to be 266 and 127 kton CO₂e [8], respectively³. The approximate construction GWP for the main tunnels are 6.38 kton CO₂e/km for CLIC (5.6m diameter) and 7.34 kton CO₂e/km for ILC (9.5m diameter); the FCC tunnel design is similar to that of CLIC, so 6.38 kton CO₂e/km is used for the calculation of emissions for both FCC and CEPC. While a comprehensive civil engineering report is unavailable for FCC and CEPC, we estimate the concrete required for klystron gallery, access shafts, alcoves, and caverns to contribute an additional 30% of emissions, similar to what is anticipated for CLIC. The analysis indicates that the A4-A5 components constitute 20% for CLIC and 15% for ILC. In the absence of equivalent life cycle assessment analysis for FCC and CEPC, we account for the A4-A5 contributions as an additional 25%. A summary of these parameters is given in Table 5.

The C³ tunnel will be about 8 km long with a rectangular profile in each of its component systems. Assuming a cut and cover approach, all the excavated material will be replaced to yield a small berm. We estimate that for the whole accelerator complex only about 50 thousands cubic meters of spoil for the experimental hall will have to be relocated. Figure 3 shows a schematic of the

²Contributions from many bypass tunnels, access shafts, large experimental caverns, and new surface sites are excluded.

³We use the emissions figures associated to the CLIC drive-beam design, which is more efficient than the alternative design utilizing only klystrons for RF power.

Table 5: Summary of GWP for different collider proposals separated by origin. Note that FCC and CEPC emissions are estimated based on the comprehensive life cycle assessment of ILC and CLIC, whereas those of ILC and CLIC are directly quoted from the report. The assumptions for the C³ estimate are discussed in the text.

Project	Main tunnel length (km)	GWP (kton CO ₂ e)		
		Main tunnel	+ other structures	+ A4-A5
FCC	90.6	578	751	939
CEPC	100	638	829	1040
ILC	13.3	97.6	227	266
CLIC	11.5	73.4	98	127
C ³	8.0	133	133	146

C³ cross section, where the klystron gallery is situated directly above the accelerator hall with sufficient concrete shielding to allow constant access to the klystron gallery during operation. The application of a top-down estimate of 6-7 kton CO₂e/km obtained from the ARUP report is not appropriate for the C³ surface site due the differing cross section geometries of the accelerator housing. To allow for a fair comparison among facilities, we take the same basic assumptions of construction materials. In particular, that construction uses a mix of CEM1 C40 concrete and 80% recycled steel, the GWP of concrete is taken to be 0.18 kg CO₂e /kg concrete with density 2400 kg/m³[33], and 85%/15% of emissions originate from concrete/steel production. Taking into account construction of the main linacs, injector linacs, damping rings, beam delivery system, and experimental hall, the total volume of construction material is estimated to be about 260,000 m³ (consisting mostly of concrete by volume). This leads to a GWP of 133 kton CO₂e for A1-A3 components and GWP per unit length of the main linac of around 17 kton CO₂e/km. Notably, this is roughly a factor 2 larger than the GWP/km of main tunnel construction of ILC and CLIC; this suggests further tunnel geometry optimizations are achievable with a detailed engineering study. The surface site construction eliminates the need for additional infrastructure (e.g. access tunnels and turnarounds) and greatly reduces the complexity of the construction process, which we estimate to account for an additional 10%⁴ to the GWP. This yields a final estimate of 146 kton CO₂e for civil engineering.

Unlike other Higgs factories under evaluation, the C³ site has not been decided yet. A C³ e⁺e⁻ collider could in principle be sited anywhere in the world. A community decision will be made regarding the actual site selection, although we note that the C³ offers a unique opportunity to realize an affordable energy frontier facility in the US in the near term and the entire program could be sited within the existing US National Laboratories. The C³ tunnel layout would be adapted to its location, and a cut and cover site, suitable for a horizontal layout, is extremely attractive also for both cost and schedule reasons. The details of the siting options at FNAL are discussed in [34]. Sites such as the

⁴This estimate is half the A4-A5 component associated to tunnelled facilities and is expected to overestimate the improvement associated to a cut and cover approach, due to significant reduction to spoil transport and operation of a boring machine

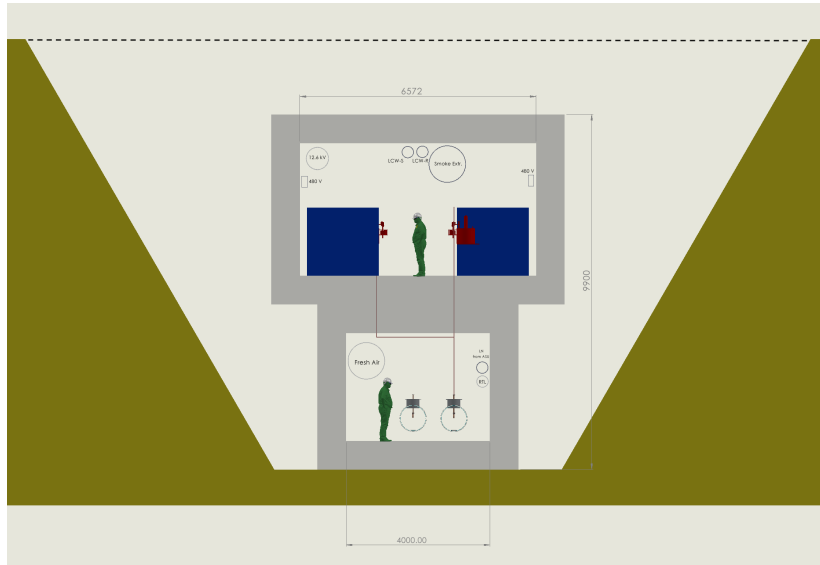


Figure 3: Layout of the C^3 klystron gallery (upper level) and accelerator hall (lower level) in the cut-and-cover construction approach, which is used for both the main linac and injectors. Key components of physical infrastructure are shown. The dashed line shows the ground level. All the excavated material will be placed to yield a small berm.

DOE Hanford site located in the Pacific Northwest have room to accommodate even bigger footprint machines within their site boundary.

6 Mitigation strategies for operations

There can be considerable emissions associated with the production of energy required to meet site operation power requirements. This is highly dependent on the region in which the project operates; regions with highly de-carbonized electricity grids (via solar, wind, hydroelectric, and nuclear power) offer significantly reduced carbon emissions related to energy production than those running on non-renewable energies (gas, oil, and coal). The total emissions of each collider project are then evaluated as the product of the total amount of energy consumed and the local carbon intensity for its production.

While total de-carbonization of the electric grid by 2040 is a nominal goal, it is not assured. The 2040 projection of carbon intensity based on the stated policies scenario for Japan, China, the European Union, and the United States are roughly 150, 300, 40, and 45 tCO_2e/GWh , respectively [35]. However, local variations in renewable energy systems implementation is neglected in these estimates; for example, the CERN-based colliders could take advantage of a 50-50 mix of renewable and nuclear energy. Additional mitigation strategies, such as construction of dedicated renewable energy plants, would reduce the carbon impact of operations in other regions. This strategy has been thoroughly investigated by the Green ILC Project [36]. A more moderate strategy can be envisioned for C^3 . A 185 MW solar farm could be built with a \$150 million budget [37], double covering the average power

requirement of C^3 ⁵, such that excess power could be stored for later use at night⁶, allowing C^3 to achieve green energy independence. The use of multi-junction photovoltaic cell fabrication techniques would improve power conversion efficiency well beyond 30% that is common in today's cells [38], allowing such a solar farm to be situated on about 5 km² of land [39].

This estimate relies on energy storage systems supported by regional electricity grids. To better understand the feasibility of scaling all parts of energy production (which may fall under the C^3 project budget) and energy storage infrastructure (which would be funded by the US government, but would nonetheless need investment), we perform a holistic cost estimate. We first note that the energy storage capacity required to supply 150 MW continuously for 12 hours is less than 1% the expected grid energy storage capacity in 2040 [40], indicating that the US grid should be able to reasonable support operations at this scale using renewable energy. We assume lithium ion batteries⁷ are the primary energy storage technology with a lifetime of 1000 cycles, experiencing 300 cycles per year with 10% of battery cost reclaimed through recycling at a base cost of 125 (100) \$/kWh in 2040 and 2050 [41]. We take the cost of energy production of solar to be \$0.80/W [39] while taking that of onshore, fixed-bottom offshore and floating offshore wind turbines to be around 1.3, 3.25 and 5.3 \$/W [42, 43]. An energy production portfolio that provides continuous power for C^3 over a 12 hour day/12 hour night period based on these technologies alone would cost approximately \$1 billion. This estimate is primarily driven by requirements of battery energy storage systems and holds for a variety of energy source mixes. This indicates a similar cost would be associated to a site located near the Pacific or Atlantic coasts, which could leverage floating and fixed-bottom turbines respectively, in the Southern US where solar would be most efficient, or proximate to large wind farms in the Midwest. A more precise cost and feasibility analysis can be performed when a candidate site is defined, as has been done for experiments operating at the South pole, for example [44]. This cost analysis demonstrates that C^3 operations could be supported sustainably within the US within the next two decades given conservative projections of technological development.

As a point of comparison, the power requirement of FCC would be about 30% of the output of a large nuclear plant (generating 1.1 GW on average [45]). At about \$8 billion per facility, the cost of renewable energy infrastructure for FCC would be about \$2.5 billion. To obtain an estimate of the carbon impact of operations at future collider facilities that takes mitigation strategies into account, we first note the carbon intensity of solar, wind, hydro, and nuclear are around 30, 15, 25 and 5 tCO₂e/GWh, respectively [46]. These estimates have some regional variation due to the differences in supply chains and local infrastructure. For instance, given the lifetime of existing nuclear plants of about 30 years, replacement or construction of entirely new facilities will be required and it might effect the overall carbon intensity. While the ultimate energy production portfolio will be different for facilities constructed in different regions, we take a common estimate of 20 tCO₂e/GWh for all collider facilities in this analysis. We find this to be a reasonable estimate given that any facility can propose

⁵This estimate considers the power optimizations in Table 4

⁶The additional cost of selling and purchasing energy through utility companies can be reduced through special contracts and is neglected here

⁷Lithium ion batteries are not considered to be viable long term energy storage solutions, instead technologies such as flow batteries and systems based on mechanical potential energy are favored

mitigation strategies to decouple their carbon impact from the regional average. It also reflects the expectation that clean energy infrastructure supply chains will improve over the next 20 years.

7 Analysis of total carbon footprint

A straightforward calculation of total energy consumption is possible using the information summarized in Table 6, which includes estimates of the site power P during collision mode, the annual collision time $T_{\text{collisions}}$ and the total running time in years T_{run} for each center-of-mass energy \sqrt{s} considered. We take into account the time spent with the beam operating at full RF and cooling power outside of data-taking mode, for example for machine development, as an additional week for every 6 weeks of data-taking (i.e. +17%), represented as $T_{\text{development}}$. We take the site power requirement for the remaining period in a calendar year to be 30% of the site power requirement during data-taking (denoted by κ_{down}). This value is a conservative upper estimate, since without RF power and associated heat load, any accelerator can be kept cold with a small fraction of power to the cryogenics system.

Table 6: For each of the Higgs factory projects considered in the 1st row, the center-of-mass energies (2nd row), AC site power (3rd row), annual collision time (4th row), total running time⁸ (5th row), instantaneous luminosity per interaction point (6th row) and target integrated luminosity (7th row) at each center-of-mass energy are given. The numerical values were taken from the references mentioned in the table in conjunction with [47]. For CEPC the new baseline scenario with 50 MW of SR power per beam is used. We consider both the baseline and the power optimizations of Table 4 (in brackets) for C³ power requirements.

Higgs factory	CLIC [48]	ILC [12]		C ³ [11]		CEPC [49],[50]				FCC [20],[51], [52]					
\sqrt{s} [GeV]	380	250	500	250	550	91.2	160	240	360	88,91,94	157,163	240	340-350	365	
P [MW]	110	111	173	150 (87)	175 (96)	283	300	340	430	222	247	273	357		
$T_{\text{collisions}}$ [10^7 s/year]	1.20	1.60		1.60		1.30				1.08					
T_{run} [years]	8	11	9	10	10	2	1	10	5	2	2	2	3	1	4
$\mathcal{L}_{\text{inst/IP}}$ [$\cdot 10^{34}$ cm ⁻² s ⁻¹]	2.3	1.35	1.8	1.3	2.4	191.7	26.6	8.3	0.83	115	230	28	8.5	0.95	1.55
\mathcal{L}_{int} [ab ⁻¹]	1.5	2	4	2	4	100	6	20	1	50	100	10	5	0.2	1.5

Using these values, the annual energy consumed is calculated as:

$$E_{\text{annual}} = P \left[\kappa_{\text{down}} \cdot T_{\text{year}} + (1 - \kappa_{\text{down}})(T_{\text{collisions}} + T_{\text{development}}) \right] \quad (7.1)$$

and the total energy consumption summing over all run configurations \sqrt{s} runs is

$$E_{\text{total}} = \sum_{r \in \text{runs}} E(r)_{\text{annual}} \cdot T_{\text{run}}(r) \quad (7.2)$$

For the circular collider projects, FCC and CEPC, we consider separately the cumulative energy consumption of the Higgs physics runs (i.e. $\sqrt{s} > 240$ GeV) for a focused comparison on the basis of Higgs physics reach argued in Section 3, but additionally include the contribution of Z -pole and WW -threshold runs which impact the climate nevertheless.

⁸The nominal run schedule reflects nominal data-taking conditions which neglect other run periods such as luminosity ramp-up.

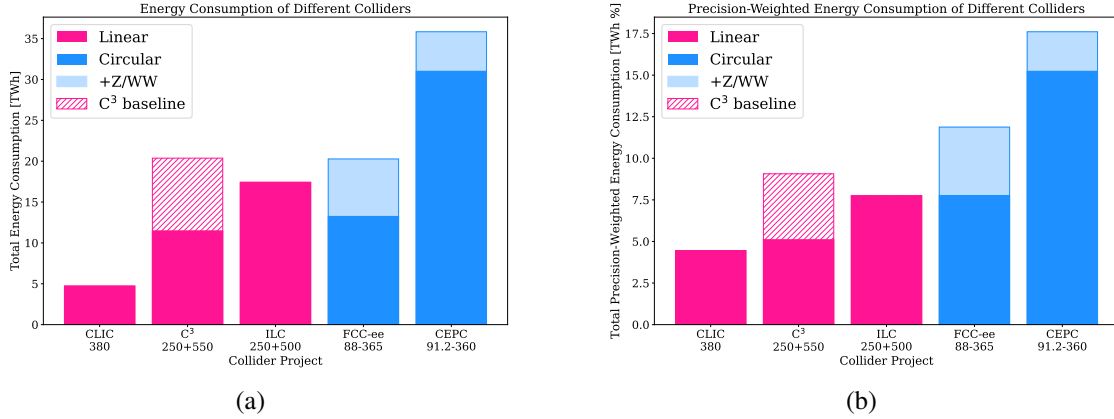


Figure 4: Total energy consumption for all collider concepts, both (a) unweighted and (b) weighted with respect to the average coupling precision for each collider. We note that the hashed pink component represents the additional costs of operating C³ without power optimisations, while light blue regions account for additional run modes targeting Z and WW production.

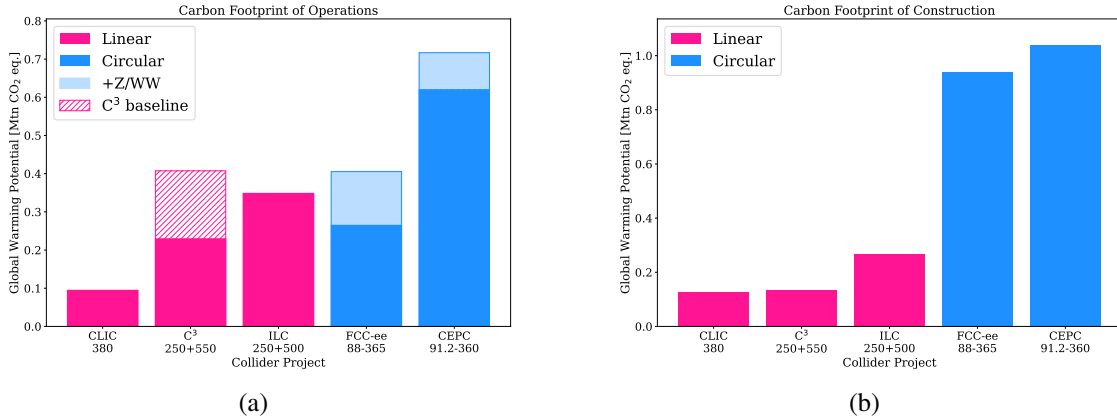


Figure 5: Global warming potential from (a) operations and (b) construction of all collider concepts. We note that the hashed pink component represents the additional costs of operating C³ without power optimisations, while light blue regions account for additional run modes targeting Z and WW production.

Figure 4a shows the energy consumption for the considered collider projects. The least energy is consumed by CLIC, driven by the lowest planned run time at low energies and its marginally lower power consumption compared to C³ and ILC, which are comparable. The energy consumption of CEPC is large compared to FCC because CEPC plans to collect four times the integrated luminosity at 240 GeV with an associated tripling of the total run duration.

Figure 4b shows the precision-weighted energy consumption for the considered collider projects,

estimated by multiplying the energy consumption of Figure 4a with the average relative precision in the last row of Table 2. The lowest run time for CLIC is now compensated by the reduced relative precision, in comparison to C^3 and ILC, leading to overall closer precision-weighted energy consumption. Similarly, the large proposed run time for CEPC is now taken into account in conjunction with the improved precision reach, yielding a total weighted energy consumption closer to FCC.

Figure 5a shows the associated GWP of the total energy required for operations, obtained by multiplying the total energy consumption by the respective carbon intensity. The GWP of FCC operations benefits from the de-carbonized electricity expected in France and Switzerland, despite its high total energy requirements.

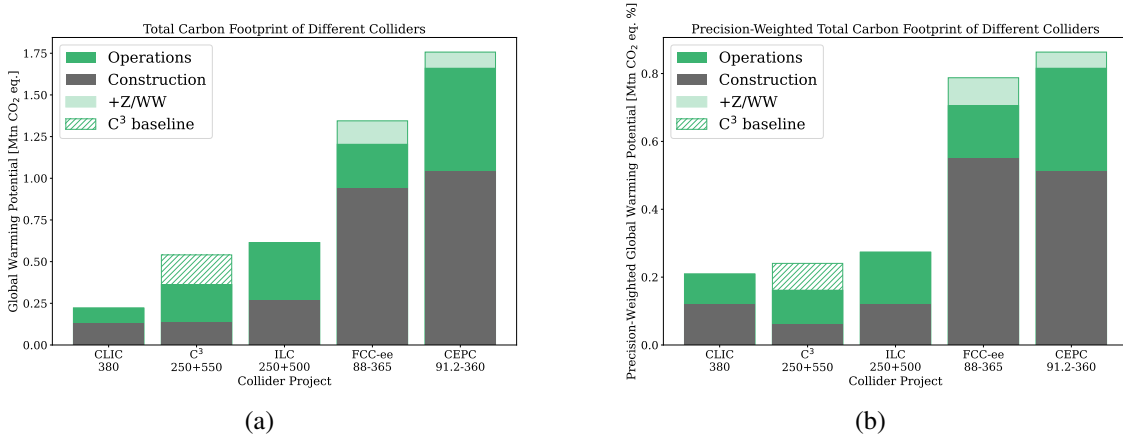


Figure 6: Total global warming potential from construction and operations for all collider concepts, both (a) unweighted and (b) weighted with respect to the average coupling precision for each collider. We note that the hashed pink component represents the additional costs of operating C^3 without power optimisations, while light blue regions account for additional run modes targeting Z and WW production.

Figure 5b shows the GWP due to construction of accelerator facilities. The carbon footprint is very similar among the linear and circular colliders, which is driven primarily by the total length of the accelerator. Figure 6a shows the total GWP from construction and operations. CLIC is the most environmentally friendly option, owing to its lead performance in operations emissions as well as its small footprint. The total GWP of C^3 and ILC are driven by operations while that of CLIC, FCC, and CEPC are almost entirely driven by construction emissions. Possible reductions in the construction component could be achieved by using concrete with lower cement content than CEM1 C40 considered in this analysis. Such cases would still leave FCC GWP dominated by construction processes.

Finally, Figure 6b shows the total precision-weighted GWP from construction and operations, estimated in the same way as the precision-weighted energy consumption in Figure 4b. Given the overall similar GWP for CLIC and C^3 and the superior precision reach of C^3 at higher energies, compared to CLIC, C^3 appears to be the most environmentally friendly option, when accounting for the precision-weighted total carbon footprint.

8 Conclusions

We present the first analysis of the environmental impact of the newly proposed C^3 collider and a comparison with the other proposed facilities in terms of physics reach, energy needs and carbon footprint for both construction and operations.

The physics reach of the proposed linear and circular e^+e^- colliders has been studied extensively in the context of the US Snowmass and European Strategy processes. We zero in on the Higgs boson coupling measurement precision achievable at C^3 , CLIC, ILC, FCC, and CEPC and point out that they are generally similar, though linear colliders can operate at higher collision energies allowing access to additional measurements of the Higgs boson's properties. Moreover, the use of polarization at linear facilities effectively compensates for the lower luminosity.

On this basis, the global warming potential of these facilities is compared in terms of absolute environmental impact and in terms of environmental impact per unit of physics output obtained by a weighted average of expected precision on Higgs coupling measurements. The operations emissions of C^3 could be improved through beam parameter optimization leading to 63 (79) MW power reduction compared to the nominal 150 (175) MW in the 250 (550) GeV running mode. Mitigation strategies using dedicated renewable energy facilities can reduce the carbon intensity of energy production to 20 ton CO_2e/GWh . We find that global warming potential is driven by construction rather than by operations beyond 2040. The compact nature of linear collider facilities reduces the total volume of construction materials and opens up the option for a surface site to simplify the construction process. We conclude that linear colliders and C^3 in particular have great potential for an environmentally sustainable path forward for high energy collider facilities.

9 Acknowledgements

The authors express their gratitude to Dan Akerib, Tom Shutt, Sridhara Dasu, Patrick Maede, and Jim Brau for their insightful discussions, which have significantly contributed to this work. The authors also extend their appreciation to Michael Peskin and Steinar Stapnes for providing feedback on the manuscript. The work of the authors is supported by the US Department of Energy under contract DE-AC02-76SF00515.

References

- [1] M. Narain, L. Reina, A. Tricoli, M. Begel, A. Belloni, T. Bose, A. Boveia, S. Dawson, C. Doglioni, A. Freitas, et al., *The Future of US Particle Physics—The Snowmass 2021 Energy Frontier Report*, [arXiv:2211.11084 \[hep-ex\]](#).
- [2] J. N. Butler et al., *Report of the 2021 U.S. Community Study on the Future of Particle Physics (Snowmass 2021) Summary Chapter*, in *Snowmass 2021*. 1, 2023. [arXiv:2301.06581 \[hep-ex\]](#).
- [3] CFA Panel for Sustainable Accelerators and Colliders Collaboration, T. Roser, *Sustainability Considerations for Accelerator and Collider Facilities*, in *Snowmass 2021*. 3, 2022. [arXiv:2203.07423 \[physics.acc-ph\]](#).
- [4] K. Bloom, V. Boisvert, and M. Headley, *Report of the Topical Group on Environmental and Societal Impacts of Particle Physics for Snowmass 2021*, [arXiv:2209.07684 \[physics.soc-ph\]](#).
- [5] K. Bloom, V. Boisvert, D. Britzger, M. Buuck, A. Eichhorn, M. Headley, K. Lohwasser, and P. Merkel, *Climate impacts of particle physics*, in *Snowmass 2021*. 3, 2022. [arXiv:2203.12389 \[physics.soc-ph\]](#).
- [6] *The Green ILC Project*, . <https://green-ilc.in2p3.fr/home/>.
- [7] P. Janot and A. Blondel, *The carbon footprint of proposed e^+e^- Higgs factories*, *Eur. Phys. J. Plus* **137** (2022) no. 10, 1122, [arXiv:2208.10466 \[hep-ph\]](#).
- [8] Suzanne Evans and Ben Castle and Yung Loo and Heleni Pantelidou, *Comparative environmental footprint for future linear colliders CLIC and ILC*, tech. rep., ARUP Group, 2023. https://indico.slac.stanford.edu/event/7467/contributions/5902/attachments/2851/7968/ARUP_CERN_LCA_LCWS_-_2023.pdf.
- [9] M. Bai et al., *C³: A "Cool" Route to the Higgs Boson and Beyond*, 10, 2021. [arXiv:2110.15800 \[hep-ex\]](#).
- [10] S. Dasu, E. A. Nanni, M. E. Peskin, C. Vernieri, et al., *Strategy for Understanding the Higgs Physics: The Cool Copper Collider*, in *Snowmass 2021*. 3, 2022. [arXiv:2203.07646 \[hep-ex\]](#).
- [11] E. A. Nanni, M. Breidenbach, C. Vernieri, et al., *C³ Demonstration Research and Development Plan*, [arXiv:2203.09076 \[physics.acc-ph\]](#).
- [12] ILC International Development Team Collaboration, *The International Linear Collider: Report to Snowmass 2021*, [arXiv:2203.07622 \[physics.acc-ph\]](#).
- [13] K. L. Bane, T. L. Barklow, M. Breidenbach, C. P. Burkhardt, E. A. Fauve, A. R. Gold, V. Heloin, Z. Li, E. A. Nanni, M. Nasr, et al., *An Advanced NCRF Linac Concept for a High Energy e^+e^- Linear Collider*, arXiv preprint [arXiv:1807.10195](#) (2018) .

- [14] M. Nasr, E. Nanni, M. Breidenbach, S. Weathersby, M. Oriunno, and S. Tantawi, *Experimental demonstration of particle acceleration with normal conducting accelerating structure at cryogenic temperature*, Physical Review Accelerators and Beams **24** (2021) no. 9, 093201.
- [15] S. Belomestnykh, E. A. Nanni, H. Weise, S. V. Baryshev, P. Dhakal, R. Geng, B. Giaccone, C. Jing, M. Liepe, X. Lu, et al., *RF Accelerator Technology R&D: Report of AF7-RF Topical Group to Snowmass 2021*, arXiv preprint arXiv:2208.12368 (2022) .
- [16] M. Schneider, V. Dolgashev, J. W. Lewellen, S. G. Tantawi, E. A. Nanni, M. Zuboraj, R. Fleming, D. Gorelov, M. Middendorf, and E. I. Simakov, *High gradient off-axis coupled C-band Cu and CuAg accelerating structures*, Applied Physics Letters **121** (2022) no. 25, 254101.
- [17] A. M. Robert Barry. <https://indico.slac.stanford.edu/event/7315/contributions/4767/>.
- [18] P. Bambade et al., *The International Linear Collider: A Global Project*, arXiv:1903.01629 [hep-ex].
- [19] T. Roser et al., *On the feasibility of future colliders: report of the Snowmass'21 Implementation Task Force*, JINST **18** (2023) no. 05, P05018, arXiv:2208.06030 [physics.acc-ph].
- [20] G. Bernardi et al., *The Future Circular Collider: a Summary for the US 2021 Snowmass Process*, 2022. arXiv:2203.06520 [hep-ex].
- [21] CEPC Accelerator Study Group Collaboration, *Snowmass2021 White Paper AF3-CEPC*, arXiv:2203.09451 [physics.acc-ph].
- [22] CLIC accelerator Collaboration, *The Compact Linear Collider (CLIC) - Project Implementation Plan*, arXiv:1903.08655 [physics.acc-ph].
- [23] S. Dawson, P. Meade, I. Ojalvo, C. Vernieri, et al., *Report of the Topical Group on Higgs Physics for Snowmass 2021: The Case for Precision Higgs Physics*, 2022. arXiv:2209.07510 [hep-ph].
- [24] T. Barklow, K. Fujii, S. Jung, R. Karl, J. List, T. Ogawa, M. E. Peskin, and J. Tian, *Improved Formalism for Precision Higgs Coupling Fits*, Phys. Rev. D **97** (2018) no. 5, 053003, arXiv:1708.08912 [hep-ph].
- [25] T. Barklow, J. Brau, K. Fujii, J. Gao, J. List, N. Walker, and K. Yokoya, *ILC Operating Scenarios*, arXiv:1506.07830 [hep-ex].
- [26] J. Cai, I. Syratchev, and G. Burt, *Design study of a high-power Ka-band high-order-mode multibeam klystron*, IEEE Transactions on Electron Devices **67** (2020) no. 12, 5736–5742.
- [27] Q. Chao, R. Zhang, Y. Wang, and X. Zhang, *Modeling and design of a high-efficiency multibeam klystron*, IEEE Transactions on Electron Devices **69** (2022) no. 5, 2625–2630.
- [28] J. Cai, I. Syratchev, and G. Burt, *Development of X-band High Power High Efficiency Klystron*, in *High Gradient Workshop, Virtual*. 2021.
- [29] *Development of X-band High power High efficiency Klystron*, . https://indico.cern.ch/event/991188/contributions/4170246/attachments/2175419/3673317/Development%20of%20X-band%2050MW%20High%20efficiency%20Klystron%20v3_upload%20version.pdf.
- [30] P. Wang, H. Zha, I. Syratchev, J. Shi, and H. Chen, *Rf design of a pulse compressor with correction cavity chain for klystron-based compact linear collider*, Physical Review Accelerators and Beams **20** (2017) no. 11, 112001.

- [31] E. Snively, V. Borzenets, G. Bowden, A. Krasnykh, Z. Li, C. Nantista, M. Oriunno, S. M Shumail, et al., *Cryogenic accelerator design for compact very high energy electron therapy*, in *Proc. LINAC*, pp. 62–64. 2022.
- [32] M. Schneider, *REBCO Sample Testing for a HTS High Q Cavity*, in *Proc. IPAC'23*.
- [33] BCSA, Steel for Life, SCI, *Lightweight C40 CEM 1 Data Sheet*, tech. rep., PE International, 2012. https://steelconstruction.info/The_Steel_Construction_Information_System.
- [34] P. C. Bhat et al., *Future Collider Options for the US*, in *Snowmass 2021*. 3, 2022. [arXiv:2203.08088](https://arxiv.org/abs/2203.08088) [hep-ex].
- [35] International Energy Agency (IEA), *World Energy Outlook 2022*, , Licence: Creative Commons Attribution CC BY-NC-SA 4.0., 2022. <https://www.iea.org/reports/world-energy-outlook-2022>.
- [36] G.-I. P. Team, *The Green ILC Project - Green ILC*, 2023. <https://green-ilc.in2p3.fr/home/>.
- [37] SEIA, *Solar Market Insight Report 2021 Q4*, 12, 2021. <https://www.seia.org/research-resources/solar-market-insight-report-2021-q4>.
- [38] T. Hunt, *How to Make Money From Land as a Solar Developer*, 8, 2013. <https://www.greentechmedia.com/articles/read/how-to-make-money-from-your-land-as-a-solar-developer#gs.66msmc>.
- [39] P. R. Brown, P. J. Gagnon, J. S. Corcoran, and W. J. Cole, *Retail Rate Projections for Long-Term Electricity System Models*, Technical Report NREL/TP-6A20-78224, National Renewable Energy Laboratory, Golden, CO, 2022. <https://www.nrel.gov/docs/fy22osti/78224.pdf>.
- [40] P. Denholm and W. Frazier, *Storage Futures Study: Economic Potential of Diurnal Storage in the U.S. Power Sector*, tech. rep., National Renewable Energy Laboratory, 2021. <https://www.nrel.gov/docs/fy21osti/77449.pdf>.
- [41] National Renewable Energy Laboratory, *Utility-Scale Battery Storage*, 2022. https://atb.nrel.gov/electricity/2022/utility-scale_battery_storage.
- [42] D. Blewett, *Wind Turbine Cost: Worth The Million-Dollar Price In 2022?*, 12, 2021. <https://weatherguardwind.com/how-much-does-wind-turbine-cost-worth-it/>.
- [43] U.S. Department of Energy, *Land-Based Wind Market Report: 2022 Edition*, 8, 2022. https://www.energy.gov/sites/default/files/2022-08/land_based_wind_market_report_2022_ppt.pdf.
- [44] S. Babinec, I. Baring-Gould, A. N. Bender, N. Blair, X. Li, R. T. Muehleisen, D. Olis, and S. Ovaitt, *Feasibility of Renewable Energy for Power Generation at the South Pole*, 2023. [arXiv:2306.13552](https://arxiv.org/abs/2306.13552) [physics.soc-ph].
- [45] *France's EDF expects six new nuclear reactors to cost 46 billion euros: Le Monde*, Reuters (11, 2019) . <https://www.reuters.com/article/us-edf-nuclear-epr/frances-edf-expects-six-new-nuclear-reactors-to-cost-46-billion-euros-le-monde-idUSKBN1XJ074>.
- [46] *Electricity Maps*, <https://www.electricitymaps.com>.
- [47] T. Roser, R. Brinkmann, S. Cousineau, D. Denisov, S. Gessner, S. Gourlay, P. Lebrun, M. Narain, K. Oide, T. Raubenheimer, J. Seeman, V. Shiltsev, J. Strait, M. Turner, and L.-T. Wang, *Report of the Snowmass 2021 Collider Implementation Task Force*, 2023. [arXiv:2208.06030](https://arxiv.org/abs/2208.06030) [physics.acc-ph].

- [48] O. Brunner, P. N. Burrows, S. Calatroni, N. C. Lasheras, R. Corsini, G. D’Auria, S. Doebert, A. Faus-Golfe, A. Grudiev, A. Latina, T. Lefevre, G. Mcmonagle, J. Osborne, Y. Papaphilippou, A. Robson, C. Rossi, R. Ruber, D. Schulte, S. Stapnes, I. Syrathev, and W. Wuensch, *The CLIC project*, 2022. [arXiv:2203.09186](https://arxiv.org/abs/2203.09186) [[physics.acc-ph](https://arxiv.org/archive/physics)].
- [49] H. Cheng, W. H. Chiu, Y. Fang, Y. Gao, J. Gu, G. Li, T. Li, Z. Liang, B. Liu, J. Liu, Z. Liu, M. Ruan, J. Shu, K. Wang, L.-T. Wang, K.-P. Xie, S. Yang, J. Yuan, K. Zhang, M. Zhang, Y. Zhang, and X. Zhuang, *The Physics potential of the CEPC. Prepared for the US Snowmass Community Planning Exercise (Snowmass 2021)*, 2022. [arXiv:2205.08553](https://arxiv.org/abs/2205.08553) [[hep-ph](https://arxiv.org/archive/hep)].
- [50] C. A. S. Group, *Snowmass2021 White Paper AF3-CEPC*, 2022. [arXiv:2203.09451](https://arxiv.org/abs/2203.09451) [[physics.acc-ph](https://arxiv.org/archive/physics)].
- [51] M. Benedikt, A. Blondel, O. Brunner, M. Capeans Garrido, F. Cerutti, J. Gutleber, P. Janot, J. M. Jimenez, V. Mertens, A. Milanese, K. Oide, J. A. Osborne, T. Otto, Y. Papaphilippou, J. Poole, L. J. Tavian, and F. Zimmermann, *FCC-ee: The Lepton Collider: Future Circular Collider Conceptual Design Report Volume 2. Future Circular Collider*, Tech. Rep. 2, CERN, Geneva, 2019. <https://cds.cern.ch/record/2651299>.
- [52] J.-P. Burnet, *Energy and Sustainability for Future Circular Collider*, . <https://indico.cern.ch/event/1202105/contributions/5434701/>.